

# Molecular Dynamics Simulations of Depth Distribution of Spin-Labeled Phospholipids within Lipid Bilayer

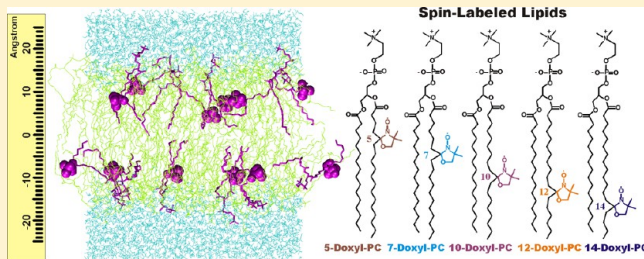
Alexander Kyrychenko<sup>\*,†,‡</sup> and Alexey S. Ladokhin<sup>†</sup>

<sup>†</sup>Department of Biochemistry and Molecular Biology, Kansas University Medical Center, Kansas City, Kansas 66160-7421, United States

<sup>‡</sup>Institute of Chemistry and School of Chemistry, V. N. Karazin Kharkiv National University, 4 Svobody Sq., Kharkiv 61022, Ukraine

**S** Supporting Information

**ABSTRACT:** Spin-labeled lipids are commonly used as fluorescence quenchers in studies of membrane penetration of dye-labeled proteins and peptides using depth-dependent quenching. Accurate calculations of depth of the fluorophore rely on the use of several spin labels placed in the membrane at various positions. The depth of the quenchers (spin probes) has to be determined independently; however, experimental determination of transverse distributions of spin probe depths is difficult. In this Article, we use molecular dynamics (MD) simulations to study the membrane behavior and depth distributions of spin-labeled phospholipids in a 1-palmitoyl-2-oleoyl-*sn*-glycero-3-phosphocholine (POPC) bilayer. To probe different depths within the bilayer, a series containing five Doxyl-labeled lipids (*n*-Doxyl PC) has been studied, in which a spin moiety was covalently attached to *n*th carbon atoms (where *n* = 5, 7, 10, 12, and 14) of the *sn*-2 stearoyl chain of the host phospholipid. Our results demonstrate that the chain-attached spin labels are broadly distributed across the model membrane and their environment is characterized by a high degree of mobility and structural heterogeneity. Despite the high thermal disorder, the depth distributions of the Doxyl labels were found to correlate well with their attachment positions, indicating that the distribution of the spin label within the model membrane is dictated by the depth of the *n*th lipid carbon atom and not by intrinsic properties of the label. In contrast, a much broader and heterogeneous distribution was observed for a headgroup-attached Tempo spin label of Tempo-PC lipids. MD simulations reveal that, due to the hydrophobic nature, a Tempo moiety favors partitioning from the headgroup region deeper into the membrane. Depending on the concentration of Tempo-PC lipids, the probable depth of the Tempo moiety could span a range from 14.4 to 18.2 Å from the membrane center. Comparison of the MD-estimated immersion depths of Tempo and *n*-Doxyl labels with their suggested experimental depth positions allows us to review critically the possible sources of error in depth-dependent fluorescence quenching studies.



## INTRODUCTION

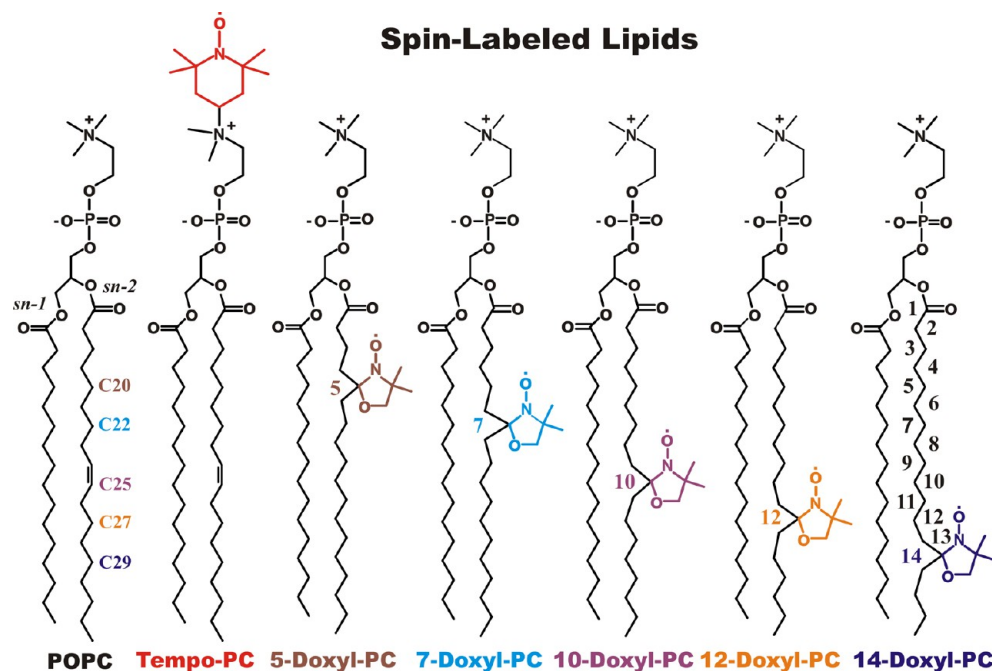
Spin-labeled phospholipids or fatty acids have often been used as spin probes in various fields of membrane biophysics.<sup>1</sup> A spin label, such as a nitroxide moiety containing a stable free radical, introduced into either the polar headgroup or the *n*th carbon positions in the host lipid chain, quenches the fluorescence of a target molecule depending on their relative proximity within the membrane. Since a spin moiety quenches only nearby fluorophores, the most efficient quenching will occur when the quencher and the fluorophore are located at the same depth in the membrane. The depth-dependent fluorescence quenching methodology has long been used in parallax<sup>2</sup> and distribution analysis<sup>3–5</sup> for measuring the depth of amino acid residues in membrane-inserted peptides.<sup>6</sup> The reliability of these approaches is crucially dependent on assumptions that lipid-attached spin quenchers are rigidly anchored at well-known depths within a membrane. Knowledge of the precise location of the spin quencher is therefore essential to interpret spectroscopic results.

Several experimental approaches have been designed to measure the depth of spin labels within a membrane by using fluorescence,<sup>2,6–8</sup> electron paramagnetic resonance (EPR),<sup>9–11</sup> nuclear magnetic resonance (NMR),<sup>12,13</sup> as well as electron-spin echo envelope modulations (ESEEM) spectroscopy.<sup>14</sup> These spectroscopic techniques have shown that overall structural and dynamics behaviors of spin-labeled lipids had many features similar to those of unlabeled PC;<sup>15–17</sup> however, high-resolution structure details were often unavailable from such experiments. It is commonly accepted that the depth of spin labels can be approximated by the depth of the corresponding carbon atoms of the unlabeled fatty acyl chain and that the depth of the labeling position can be inferred from a rigid, all-trans configuration of the lipid acyl chains.<sup>2,9</sup> The widely accepted depth calibration scale<sup>9</sup> is based on the all-trans conformation of *sn*-2 acyl chain of dimyristoyl-PC crystals,

Received: March 17, 2013

Revised: April 20, 2013

Published: April 24, 2013

Scheme 1. Molecular Structure of Spin-Labeled Lipids<sup>a</sup>

<sup>a</sup>Structure and atom numbering of unlabeled POPC, Tempo-PC (1-palmitoyl-2-oleoyl-*sn*-glycero-3-phospho(TEMPO)choline), *n*-Doxyl-PC (1-palmitoyl-2-stearoyl-(*n*-Doxyl)-*sn*-glycero-3-phosphocholine) spin-labeled lipids. A Tempo label (in red) is covalently attached to a headgroup, and a Doxyl moiety (color-coded) is introduced to a variety of positions down to the *sn*-2 stearoyl chain of the host lipid.

derived from the earlier X-ray diffraction data by Pearson and Pascher<sup>18</sup> and refined according to the carbon atom positions estimated from <sup>2</sup>H NMR data of Seelig and Seelig.<sup>19</sup>

The modern view of the lipid membrane shows the inherent disorder and high mobility of the lipid acyl chain region in the liquid-crystalline phase state.<sup>20,21</sup> Therefore, the lipid membrane can no longer be considered a rigid, well-ordered environment. Indeed, more recent <sup>1</sup>H NMR studies combined with magic angle spinning (MAS) have revealed the high transverse mobility and high degree of molecular disorder of chain-attached Doxyl labels in liquid-crystalline POPC membranes.<sup>22</sup> In addition, the EPR method<sup>22</sup> had reported rather wide transverse distribution profiles of lipid-attached spin-labels. Thus, over the past few years, evidence has accumulated indicating that when a small spin quencher is attached to a lipid chain, it becomes subject to the same dynamics and high mobility as the rest of the lipid acyl chain.

The combination of experiments and molecular dynamics (MD) simulations has now become an established tool for studying the structure and dynamics of lipid membranes, adding atomistic resolution to structural data derived from X-ray and NMR studies.<sup>23–26</sup> Fluorescence techniques combined with MD simulations have been used successfully for studying the effect of hydration<sup>27,28</sup> and solvent penetration<sup>29,30</sup> on membrane properties.<sup>31–33</sup>

One of our long-term research goals is to develop integrated fluorescence spectroscopy and computational techniques for studying membrane penetration depths and topology information for membrane proteins. Recently, we used MD simulations to validate depth-dependent fluorescence quenching of tryptophan octyl ester (TOE) in a POPC bilayer.<sup>34</sup> In those simulations, we treated the unlabeled carbon atoms of the lipid acyl chain of POPC as “pseudo-quenchers” of TOE fluorescence. This approach for dynamic fluorescence quench-

ing allowed us to calculate appropriate transverse overlaps and collision rates between the quenchers and TOE. In the present work, we used MD simulations to address and refine the depth position of “real quenchers”, namely, a series of lipid-attached spin-quenchers (Doxyl and Tempo labels, Scheme 1) embedded into a POPC bilayer.

A goal of our study is to estimate the membrane depth of the Doxyl spin label attached to 5, 7, 10, 12, and 14 carbon atoms of the *sn*-2 stearoyl chain of the host phospholipid. In order to extend the depth range of quenchers into the interfacial region of the bilayer, we also examined the location of the Tempo spin moiety attached to the lipid headgroup. The MD-estimated depth positions of the lipid-attached *n*-Doxyl and Tempo spin labels are, therefore, discussed in terms of refining the depth scales that are currently used for depth-dependent fluorescence quenching studies.

## METHODS

**Molecular Dynamics Simulation Setup.** Tempo-PC and *n*-Doxyl-PC lipids (Scheme 1) were studied in a 1-palmitoyl-2-oleoyl-*sn*-glycero-3-phosphocholine (POPC) bilayer. MD simulations were performed on six different membrane systems. The initial configuration of an equilibrated POPC bilayer composed of 128 lipids was used from our previous studies.<sup>31,35</sup> In each system, either 12 or 32 lipids molecules were randomly selected for spin probe labeling. To prepare the initial configurations, we first selected an equal number of the lipids, randomly located from the upper and lower leaflets of an equilibrated POPC bilayer. Second, each *n*-Doxyl-PC spin-labeled system was prepared by direct introduction and attachment of the Doxyl label into the equilibrated POPC bilayer in water. The spin labels were attached to the corresponding carbon atom of the *sn*-2 lipid chain of POPC molecules (Scheme 1). The double bond in the *sn*-2 acyl chain

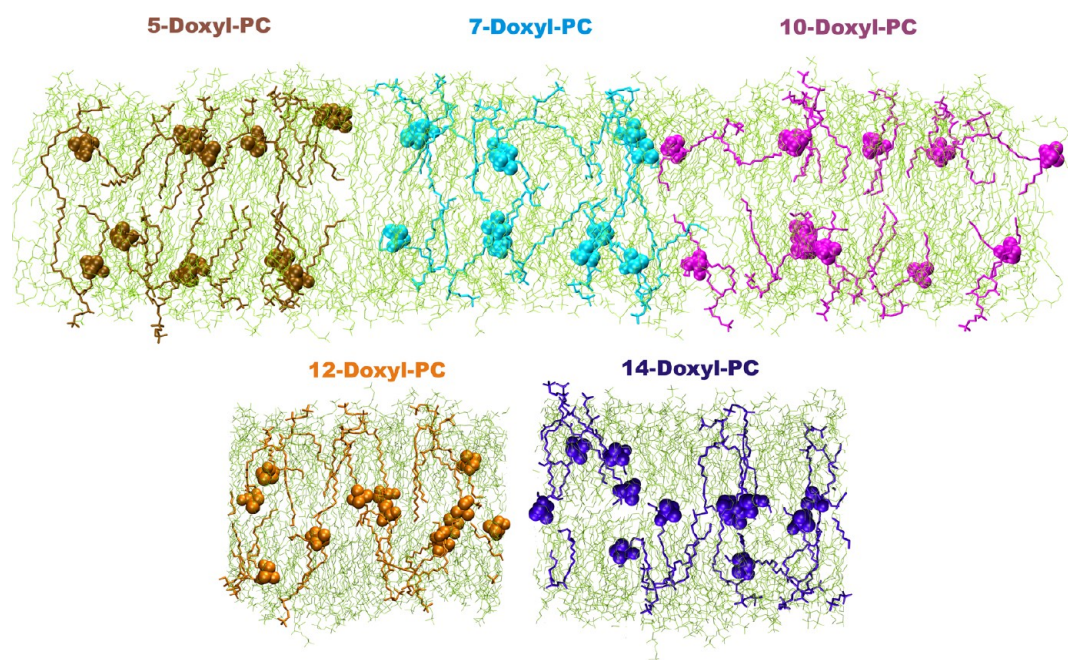


**Figure 1.** Distribution of *n*-Doxyl-PCs. Snapshots of a lipid bilayer containing 12 *n*-Doxyl-PC and 116 POPC molecules (11 mol % of bilayer spin labeling) taken at the end of MD simulations ( $t = 100$  ns). The acyl chain-attached Doxyl labels revealed the high degree of mobility and structural heterogeneity in the bilayer. The bilayer is shown as sticks in olive and *n*-Doxyl-PCs are color-coded. The Doxyl moieties are shown with van der Waals representation. Water molecules are not shown for clarity.

of POPC was removed so that the acyl chain was transformed from oleoyl to stearoyl. The initial configurations of the Tempo-PC labeled systems were prepared using the same protocol: either 12 or 32 lipids (this corresponds to 11 and 28 mol % of Tempo-PC) were selected from the upper and lower leaflets of the equilibrated POPC bilayer, and the Tempo group was covalently attached to the choline moiety of the selected POPC lipid molecules. The spin labels were inserted into a bilayer one by one, so that, after each addition, unfavorable interatomic contacts could be removed by steepest descent energy minimization and a short MD re-equilibration for 100 ps. All systems were hydrated with 4217 water molecules (lipid-to-water ratio 1:33). The initial membrane systems were equilibrated for 10 ns. After that, the final MD simulation sampling was carried out for *n*-Doxyl-PC and Tempo-PC systems for 100 and 200 ns, respectively.

A MD force field of a POPC bilayer was based on the parameters presented by Berger et al.<sup>36</sup> In POPC and spin-labeled lipids, all carbon atoms of  $\text{CH}_2$  and  $\text{CH}_3$  groups with nonpolar hydrogen atoms were treated as united atoms. For Tempo-PC and *n*-Doxyl-PC lipids, we used the same force field parameters as for POPC. The bond length and angle parameters for the Tempo and Doxyl probes were optimized by density functional theory calculations at the UB3LYP/cc-pVDZ level. Partial charges needed for Coulomb interactions were derived from the UB3LYP/cc-pVDZ electron densities by fitting the electrostatic potential to point (ESP) charges. MD topologies of the spin-labeled bilayers are available in the Supporting Information. The Simple Point Charge (SPC) model<sup>37</sup> was used for water. MD simulations were carried out at a constant number of particles, constant pressure of  $P = 1$  atm, and constant temperature  $T = 303.15$  K (NPT ensemble). Three-dimensional periodic boundary conditions were applied with the  $z$  axis lying along a direction normal to the bilayer. The pressure was controlled semi-isotropically, so that the  $x$ - $y$  and

$z$  dimensions of the simulation box were allowed to fluctuate independently from each other, keeping the total pressure constant. Thus, during MD simulations, the membrane area and thickness were therefore free to adjust under the NPT condition. The reference temperature and pressure were kept constant using the Berendsen weak coupling scheme<sup>38</sup> with a coupling constant of  $\tau_T = 0.1$  ps for the temperature coupling and  $\tau_{P(x-y)} = \tau_{P(z)} = 1.0$  ps for the pressure coupling. Electrostatic interactions were simulated with the particle mesh Ewald (PME)<sup>39</sup> approach using the long-range cutoff of 1.4 nm. The cutoff distance of Lennard-Jones interactions was also equal to 1.4 nm. All bond lengths were kept constant using the LINCS routine.<sup>40</sup> The MD integration time step was 2 fs. The MD simulations were carried out using the GROMACS set of programs, version 4.5.5.<sup>41</sup> Molecular graphics and visualization were performed using VMD 1.8.6.<sup>42</sup>

## RESULTS AND DISCUSSION

**Behavior of *n*-Doxyl-PCs in Bilayer.** To study the membrane behavior of a Doxyl spin label attached down along the stearoyl lipid chain, five different *n*-Doxyl-PC/POPC bilayer systems were prepared. Each system contained 12 molecules of *n*-Doxyl-PC lipids randomly distributed in a bilayer composed of 116 POPC lipids (where  $n = 5, 7, 10, 12, 14$ , and indicates the attachment position of the acyl chain carbon atom as shown in Scheme 1). The systems composed of *n*-Doxyl-PC/POPC lipids with a ratio of 12:116 correspond to 11 mol % of the bilayer spin labeling. This concentration is within typical concentration ranges used in depth-dependent fluorescence quenching experiments.<sup>2,8</sup> To estimate the favorable equilibrium penetration depth for spin labels in a membrane, all the *n*-Doxyl-PC labeled systems were simulated for 100 ns.

Figure 1 shows MD snapshots of typical distribution of the Doxyl-labeled lipids observed at the end of the MD sampling.



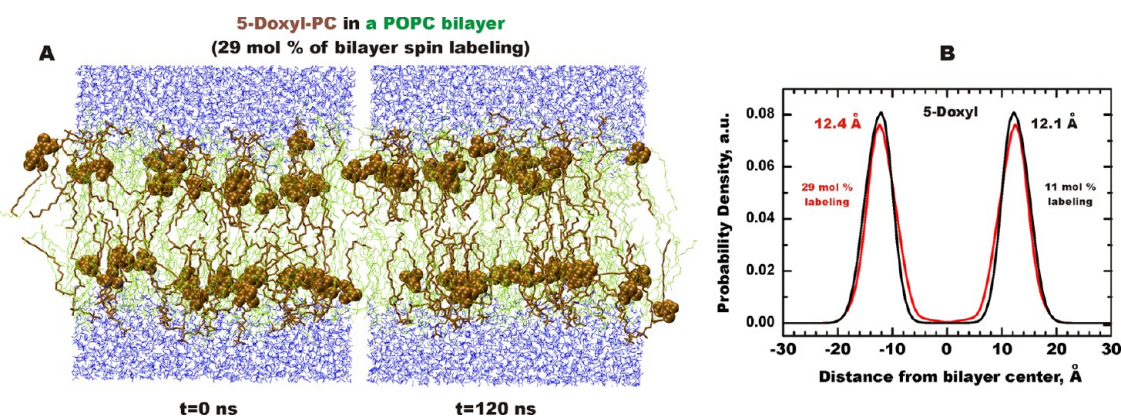


**Figure 2.** Distribution of 5-Doxyl-PC. (A) MD snapshots of lipid bilayers composed of 5-Doxyl-PC and POPC with a ratio of 34:94 (29 mol % of bilayer spin-labeling). The bilayer shown in stick representations are olive, and the 5-Doxyl-PC lipids are brown. The Doxyl labels are shown using van der Waals representation. (B) Probability densities of 5-Doxyl label shown for two different spin label concentrations of 11 (black) and 29 (red) mol %, respectively. Probability density peaks calculated from the center of a POPC bilayer are also shown.

The corresponding center-of-mass (COM) distance dynamics, averaged for spin moieties from the upper and lower leaflets, are given in Figure S2B in the Supporting Information. Depending on the attachment position, the spin labels were characterized by different degrees of COM movements. The spin moieties attached to chain carbon atoms 5 and 7 show narrow COM distributions around the certain depth within a bilayer, whereas the labels attached to carbons 12 and 14 revealed broad and high-amplitude displacements along the bilayer normal, as seen from Figure 1 and Figure S2B in the Supporting Information.

Control MD simulations for the 5-Doxyl-PC labeled bilayer also show that the penetration depth and distribution width of the Doxyl moieties were not significantly affected by the larger spin-label concentration (34:94 Doxyl-PC:POPC) up to 29 mol % (Figure 2). In addition, we noticed that the incorporation of 12 molecules of *n*-Doxyl-PC into the bilayer does not change the overall bilayer structure and results in only a small increase in the surface area. This effect becomes noticeable, however, after the insertion of 34 molecules of 5-Doxyl-PC, leading to an increase in the bilayer surface area up to 7%. It has been reported that some amphiphilic host molecules could segregate into hydrophobic and hydrophilic domains in membranes at high concentrations.<sup>43</sup> Our studies demonstrate that despite the changes in surface area, there is no phase segregation or noticeable clustering of 5-Doxyl-PC lipids in the bilayer even at concentrations of 29 mol %.

The earlier MD simulations of the nitroxide label attached to the hydrocarbon tail of stearic acid have also shown that the Doxyl groups introduced to 5-C, 10-C, and 16-C tail positions were characterized by different mobilities, and overall probe distributions within a membrane were also broad.<sup>44,45</sup> MD simulations of the localization and favorable conformations of alkyl chain-attached Doxyl labels have revealed that the anchoring properties of the host molecules in a lipid bilayer depend on the labeling position of the spin moiety.<sup>44–46</sup> When the Doxyl group was attached to the chain close to either a phosphate group or the terminal methyl, it remained well anchored at specific depths within the membrane; however, if the same group was introduced to the middle of the alkyl chain, it perturbed an extended conformation of the chain and moved closer to the interface region in the membrane. Furthermore, it was also demonstrated that the labeled molecules were even able to make flip-flop transitions between the leaflets of the

bilayer.<sup>46</sup> As has also been demonstrated for different fluorescent-labeled lipids, the location of large polar probes often reflects their intrinsic properties rather than the structure and behavior of lipid molecules to which they are attached.<sup>47–51</sup> For example, it has been shown by using both experiments and MD simulations that the presence of a polar NBD fluorophore could cause backfolding of the entire lipid chain toward the membrane interface.<sup>8,52,53</sup> Our MD simulations of the *n*-Doxyl-PC lipids show no such flip-flop transitions, suggesting that the phospholipid host molecules are able to anchor the nitroxide label at specific depths in the membrane.

**Depth of Spin Labels in the Bilayer.** The precise depths for the spin labels in the membrane were calculated using their transverse mass density profiles as shown in Figure 3A. For comparison, the decomposition of the overall mass density of the POPC bilayer into the contributions from different components: phosphate groups ( $\text{PO}_4$ ) and acyl chain *n*-carbon atoms are also presented in Figure 3B. The distribution profiles of the *n*-Doxyl labels (where *n* varies from 5-C to 10-C) were found to be as broad as the average distribution widths of the *n*-carbon atom of the lipid acyl chain to which they are attached. As labeling positions move further down the lipid chain (12-C and 14-C) toward the terminal methyl group, the transversal distribution broadening increases systematically. The Doxyl groups attached at the end of the lipid chain and, hence located deeper in the membrane, are more flexible and have more degrees of mobility.

The summary of the transverse positions of the lipid-attached spin labels in the bilayer is presented in Table 1. In the field of depth-dependent analysis, two depth scales are used that differ in their center of the origin: (i) one is centered at the center of the bilayer and ranged toward the position of the label,<sup>2–4</sup> (ii) the second is centered at the bilayer surface (assigned to peaks of phosphorus atoms of phospholipids) and ranged toward the position of the spin label.<sup>1,9,14</sup> This is why the comparison of the MD depths of the Tempo and Doxyl probes estimated within these two different depth scales is also given in Table 1. Both depth scales are, therefore, dependent on the bilayer thickness.

As indicated above, the surface positions of the upper and lower leaflets of the bilayer are commonly taken from the bilayer thickness, which can be calculated from the distance between the two distribution peaks of the phosphate group as shown in Figure 3B. In our simulations, the thickness of the

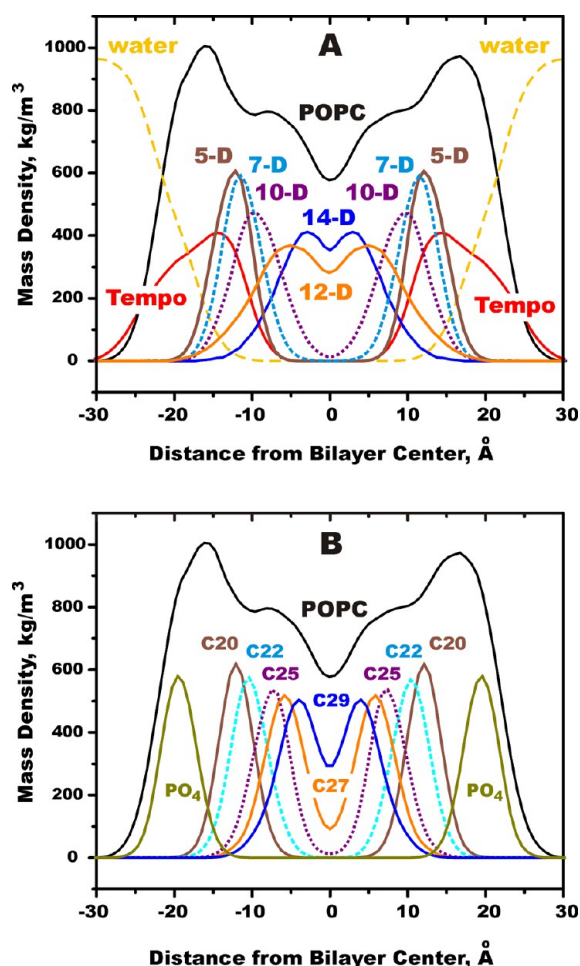


**Figure 3.** Spin label depths. Transverse mass density distributions of Tempo-PC and *n*-Doxyl-PCs in a POPC bilayer observed in MD simulations. The distributions of individual components are averaged over the last 50 ns of the MD sampling and superimposed on the profiles of a POPC bilayer (solid black) and water (dashed yellow). (A) Contributions from the spin label moieties are shown color-coded: Tempo (solid red); 5-D, 5-Doxyl (solid ochre); 7-D, 7-Doxyl (dashed cyan); 10-D, 10-Doxyl (dotted green); 12-D, 12-Doxyl (solid orange); 14-D, 14-Doxyl (solid blue). The spin label profiles were multiplied by a factor of 15 for clarity. (B) Contributions from individual components of the POPC lipids: phosphate groups, PO<sub>4</sub> (solid dark yellow), and carbon atoms of the *sn*-2 acyl chain C20, C22, C25, C27, C29 (see Scheme 1 for atom numbering). The profiles for the carbon atoms use the same coloring scheme as in panel (A).

unlabeled POPC bilayer was found to be 39.0 Å as compared to the experimental value of 37.6 Å.<sup>21</sup>

To evaluate the role of force-field parameters of the Doxyl group in favoring its penetration depths, control MD simulations were carried out for the 10-Doxyl-PC/POPC system in which electric charges at the Doxyl atoms were scaled down by a factor 10. It appears that the electrostatic contributions of the Doxyl labels have small effects on overall mobility and transverse distributions of the spin labels across a bilayer (Supporting Information Figure S1).

**Behavior of Tempo-PC in Bilayer.** To study the behavior of the headgroup-labeled lipids and the penetration depth of a Tempo spin label within a membrane, we simulated two POPC bilayer systems containing different molar percentages of Tempo-PC lipids. The systems were composed of Tempo-PC/POPC lipids with a ratio of 12:116 and 32:96 that

correspond to the bilayer spin labeling of 11 and 28 mol %, respectively. The details of the preparation of the initial systems Tempo-PC/POPC were given in Methods. The Tempo-PC/POPC systems were simulated at NPT conditions to monitor the equilibrium distribution of the Tempo labels within the bilayer. During MD sampling, the Tempo-PC lipids were driven by free thermal diffusion within the bilayer.

Figure 4A and B shows MD snapshots of the systems containing 12 and 32 Tempo-PC molecules, respectively, taken at different simulation times. As can be seen, at the beginning of the MD sampling, most Tempo labels were initially facing toward bulk water. During the initial sampling period, the spin labels gradually moved toward the bilayer surface (the middle panels in (A) and (B)). Finally, they become buried deeper into the bilayer at the end of the sampling.

To monitor system equilibration and the convergence of the probe distribution, time evolution of the center-of-mass (COM) of the Tempo labels, averaged over the probes located on the upper and lower leaflets, was plotted as a function of MD sampling time (Supporting Information Figure S2A). During the first 110–120 ns, the COM distances of the Tempo labels (calculated from the bilayer center) moved slowly from the initial positions of ~25 Å to positions deeper into the bilayer, approaching some plateau at ~14–16 Å. This time period was required for the Tempo labels to reach the equilibrium positions in the membrane and, therefore, it was discarded and excluded from further analysis. Figure 4 shows that at the equilibrium state the Tempo labels were still broadly distributed across the bilayer normal, so that a major population of the labels penetrated deeply into the hydrophobic region, whereas some fraction still favored residing at the membrane interface (Figure 3A).

The mass density profiles of the Tempo labels, calculated along the bilayer normal for the two different concentrations of Tempo-PC, are shown in Figure 5. For the 11 mol % bilayer labeling, the major density peak of Tempo was observed at 12.9 Å. Despite the long MD sampling ensuring the convergence of the average COM distance of the Tempo labels after 150 ns (Supporting Information Figure S2A), some subpopulation of the Tempo labels still exists at the membrane interface (~30 Å). In the case of the 28 mol % labeling, the distribution becomes broadened and the density peak was shifted to 15.4 Å. Taking into account the asymmetry of the distribution peaks, the most probable depths of Tempo were alternatively estimated from the center-of-weight of the distribution profiles and found to be 14.4 and 18.2 Å for the bilayer labeling of the 11 and 28 mol %, respectively (Figure 5).

**Diffusion of Doxyl Group.** The favorable residence of a solute molecule within a certain region of a membrane is often driven by physical properties of the lipid environment such as polarity, density, local viscosity as well as free volume.<sup>54</sup> The diffusion coefficient of a solute has been found to depend strongly on position and diffusion direction in the membrane. Diffusion in chain-like solvents such as lipid bilayers is also known to be related to lipid internal motions, such as overall rotation and local *trans/gauche* interconversions along the lipid hydrocarbon chains. The internal dynamics of the lipids are therefore thought to be the main mechanism responsible for free volume redistribution inside the membrane.<sup>55</sup>

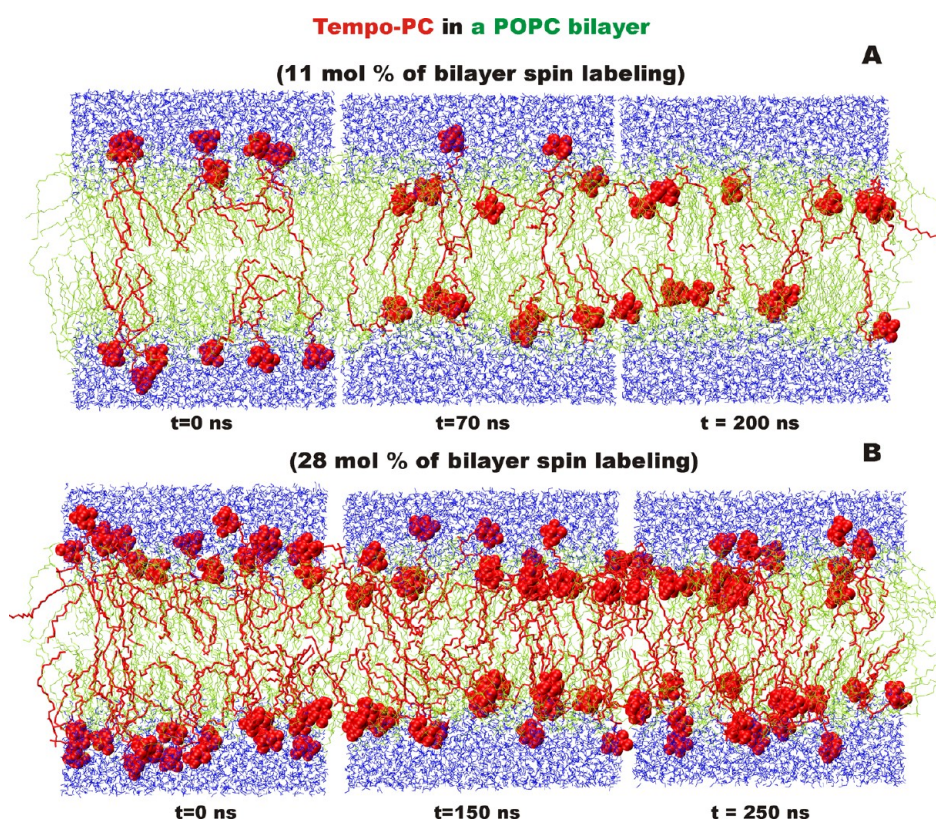
To estimate local mobility of the lipid-chain-attached Doxyl spin probes, we calculated the displacement correlations function for the self-diffusion of the Doxyl probe along the XY- and Z-dimensions within the POPC bilayer. From the



**Table 1.** MD-Estimated Depths (in Å) of the Spin Labels in a POPC Bilayer Compared with the Immersion Depths Derived by Using Various Experimental Techniques

	Tempo-PC	5-Doxyl-PC	7-Doxyl-PC	10-Doxyl-PC	12-Doxyl-PC	14-Doxyl-PC
	from center of bilayer					
	MD simulation (average position $\pm$ distribution width)					
spin label group <sup>a</sup>	18.2 $\pm$ 4.9	12.1 $\pm$ 3.0	11.5 $\pm$ 3.0	10.1 $\pm$ 3.8	6.4 $\pm$ 4.7	2.9 $\pm$ 4.8
N-O spin group	17.4 $\pm$ 4.4	12.8 $\pm$ 2.9	11.9 $\pm$ 2.9	10.0 $\pm$ 3.4	6.2 $\pm$ 4.1	3.0 $\pm$ 4.2
spiro-carbon atom of the host phospholipid		12.1 $\pm$ 2.5	10.4 $\pm$ 2.6	9.3 $\pm$ 2.8	5.5 $\pm$ 3.6	3.8 $\pm$ 3.4
<i>sn</i> -2 carbon lipid atoms in a POPC bilayer		12.1 $\pm$ 2.6	10.5 $\pm$ 2.6	7.5 $\pm$ 2.9	5.8 $\pm$ 2.9	3.6 $\pm$ 3.4
<i>sn</i> -1 carbon lipid atoms in a POPC bilayer		11.4 $\pm$ 2.6	9.9 $\pm$ 2.6	7.0 $\pm$ 2.8	4.8 $\pm$ 2.9	2.6 $\pm$ 3.2
	experiment					
X-ray diffraction <sup>b</sup>	11.1–13.1	11.0	8.6	4.6	2.1	0.1
X-ray data scaled with NMR <sup>9,c</sup>	11.1–13.1	11.0	8.6	5.1	3.1	1.8
solid-state NMR <sup>13,d</sup>		12.4		10.7		7.0
parallax analysis <sup>2,8</sup>	19.5	12.15		7.65	5.85	
	Tempo-PC	5-Doxyl-PC	7-Doxyl-PC	10-Doxyl-PC	12-Doxyl-PC	14-Doxyl-PC
	from surface of bilayer					
	MD simulation (average position $\pm$ distribution width)					
spin label group <sup>e</sup>	4.2 $\pm$ 4.9	7.5 $\pm$ 3.0	8.1 $\pm$ 3.0	9.5 $\pm$ 3.8	13.2 $\pm$ 4.7	16.7 $\pm$ 4.8
	experiment					
X-ray diffraction <sup>b</sup>	6–8	8.1	10.5	14.5	17	22
X-ray data scaled with NMR <sup>9,c</sup>	6–8	8.1	10.5	14.0	16.0	18.6
solid-state NMR <sup>13,d</sup>		10.6		12.3		16.0

<sup>a</sup>Deviation ( $\pm$ ) of the depth (in Å) corresponds to the half-width at half-height of the distribution peak. <sup>b</sup>The distances for the *sn*-2 acyl chain in the all-trans conformation of DMPC crystals were calculated from the polar surface of the bilayer (phosphorus = 0) based on X-ray diffraction data.<sup>18</sup> These distances were recalculated from the center of the POPC bilayer assuming the surface is located at 19.1 Å from the bilayer center.<sup>21</sup> The position of 14-Doxyl was taken as the average between those of 12-Doxyl and 16-Doxyl. <sup>c</sup>Distances were calculated from the X-ray diffraction results<sup>18</sup> and scaled according to the order parameter versus *sn*-2 carbon data derived from <sup>2</sup>H NMR data.<sup>9,19</sup> <sup>d</sup>Estimated from the center of a PSPC bilayer assuming the thickness of 46 Å. <sup>e</sup>The position of the phosphate group estimated in our MD simulations is at 19.6 Å the bilayer center.

**Figure 4.** Distribution of Tempo-PC. MD snapshots of lipid bilayers composed of Tempo-PC and POPC with a ratio of 12:116 (top) and 32:96 (bottom) that correspond to 10.9 and 28 mol % of bilayer spin-labeling, respectively. The bilayer shown in stick representations are olive, and the Tempo-PC lipids are red. The Tempo moieties are shown using van der Waals representation.

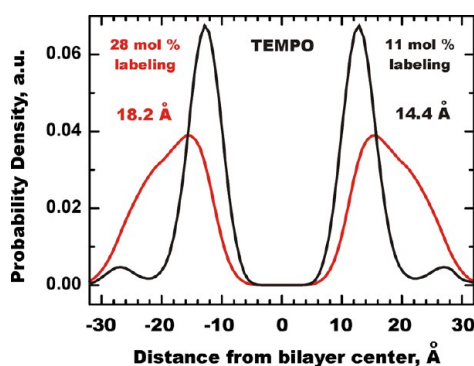


**Figure 5.** Depth of Tempo-PC. Probability densities of the Tempo label are compared for two different concentrations of 11 (black) mol % and 28 (red) mol %, respectively. To account for different concentrations, the areas under mass density profiles were normalized to 1. Due to the asymmetry of the density distributions, the most probable depth of the spin label was calculated from the center-of-weight (COW) of their probability profiles. The corresponding COW depths calculated from the center of a POPC bilayer were found to be 14.4 and 18.2 Å, respectively.

COM displacement of the Doxyl spin group calculations, the lateral ( $XY$ ) and normal ( $Z$ ) diffusion coefficients  $D_{xy}$  and  $D_z$  were estimated. Supporting Information Figure S3 shows the COM displacement of the Doxyl spin groups of a series of  $n$ -Doxyl-PC lipids along the  $Z$ -dimension of the POPC bilayer. Table 2 summarizes diffusion coefficients  $D_{xy}$  and  $D_z$ .

**Table 2.** Diffusion Coefficients of the Doxyl Spin Probe in  $n$ -Doxyl-PC Lipids Incorporated into the POPC Bilayer

spin probe	$D_{xy}$ ( $\times 10^{-7}$ cm <sup>2</sup> /s)	$D_z$ ( $\times 10^{-7}$ cm <sup>2</sup> /s)
5-Doxyl	0.350	0.030
7-Doxyl	0.440	0.115
10-Doxyl	0.495	0.190
12-Doxyl	0.560	0.240
14-Doxyl	0.680	0.320

As can be seen from Table 2, the lateral diffusion of the Doxyl moiety depends strongly on diffusion direction within the bilayer, being faster in the lateral  $X$ – $Y$  direction. The diffusion  $D_z$  occurring normal to the bilayer is slower and strongly modulated by the attachment position of the spin group along the stearyl chain, ranging from  $0.03 \times 10^{-7}$  to  $0.32 \times 10^{-7}$  cm<sup>2</sup>/s. The Doxyl labels attached close to the terminal methylene carbons of the stearyl chain diffuse faster by jumping between the free volume pockets available in the middle of the bilayer, which is in fact the lowest-density region of the system (Figure 3). The latter can explain the significant broadening of the transverse mass density of the Doxyl probes attached to C-12 and C14 carbon atoms, as observed in Figure 3.

The values of the lateral diffusion coefficients of the Doxyl probes compare favorably with experimental data ( $0.5 \times 10^{-7}$  to  $1.5 \times 10^{-7}$  cm<sup>2</sup>/s) for the lateral self-diffusion of lipid molecules in the liquid-crystalline POPC bilayer measured with fluorescence recovery after photobleaching<sup>56</sup> and fluorescence correlations spectroscopy.<sup>57</sup> These values are also in agreement with the lateral diffusion coefficient estimated for a POPC bilayer by published MD simulations.<sup>58,59</sup> Our findings indicate that the lateral diffusion of the spin probes is mainly dictated by local viscosity of the bilayer and the self-diffusion of the whole

host lipid molecule. In contrast, the overall diffusion of the Doxyl moiety along the bilayer normal appears to be restricted (Table 2).

**Reorientational Dynamics of Spin Labels.** Quenching of the electronically excited fluorophore by lipid-attached spin quenchers is a dynamic process induced by collisions between the fluorophore and the quenchers. Because of the conformational flexibility of the lipid chains and thermal diffusion, the spin probes in the membrane are the subject to rotational reorientation and diffusive motions about the membrane normal. Therefore, in addition to the self-diffusion of the Doxyl moiety, the reorientation dynamics of the spin groups were calculated from a rotation autocorrelation function (RACF)  $\langle C_2(t) \rangle$  (eq 1).<sup>60</sup>

$$\langle C_2(t) \rangle = \frac{2}{5} \left\langle \frac{3\cos^2(\cos(\Theta(t)) - 1)}{2} \right\rangle \quad (1)$$

where  $\theta(t)$  is the angle between two vectors oriented normal to the average molecular plane of the spin probe and monitored at times  $t$  and  $t + \Delta t$ , respectively.

For all the simulated spin-labeled bilayer systems, the RACFs revealed complex nonexponential decays (Figure 6). The RACFs could be well-fitted to a double exponential function (eq 2), where the fast and slow decay constants can be attributed to pseudoaxial rotation and diffusive motion of the probe.<sup>61</sup>

$$y = y_0 + A_1 \exp(-x/\tau_1) + A_2 \exp(-x/\tau_2) \quad (2)$$

Figure 6 shows that the reorientation dynamics of the spin moieties occurs on a nanosecond time scale. There is a

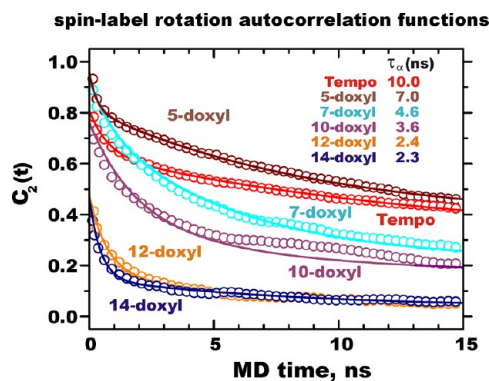


**Figure 6.** Reorientational dynamics of spin labels. Rotation autocorrelation functions for the spin label group of Tempo-PC and  $n$ -Doxyl PC in a POPC bilayer. Rotational times  $\tau_\alpha$  were calculated from fitting  $C_2(t)$  to a two-exponential decay (solid lines) and averaging fast and slow components.

systematic decrease in the time scales for the diffusive reorientation of the probe with depth into the membrane ongoing from the 5-position spin label to the 14-position label in the lipid chain. The increased rates of the reorientation dynamics down the lipid chain indicate to a progressive increase in the degree of mobility of the spin group. The Doxyl moieties attached to the terminal part of the chain (12-C and 14-C) are therefore undergoing pseudoaxial rotation on a time scale of  $\sim 2.5$  ns, whereas those attached to the lipid headgroup and the upper part of the lipid tail (5-C and 7-C) remain relatively rigidly fixed by the membrane environment on this time scale.



Our findings of the progressive increase in the degree of mobility of the Doxyl probes located deeper into the membrane are consistent with the increase in relaxation times  $\tau$  characterizing lipid internal motions within a bilayer.<sup>61</sup> The relaxation processes are thought to be related to *trans/gauche* interconversions, so that the mean life of *trans* and *gauche* conformers decreases rapidly on going from the upper part of the lipid chains toward the terminal methyl part.<sup>61</sup>

Moreover, Håkansson and co-workers<sup>60</sup> have performed MD simulations of EPR slow-motion spectra and the reorientational correlation functions of spin labeled phospholipids in liquid crystalline bilayers and found that the relaxation of the spin probes become faster closer to the end of the acyl lipid chains. Instead of the spin probes, however, they have simulated the reorientational dynamics of a vector defined by two carbon atoms on the acyl chain of DPPC lipids. To our knowledge, only a few MD simulations of lipid-attached spin labels in a bilayer are found in the literature. The nitroxide group attached to the hydrocarbon tail of stearic acids in a DPPC bilayer have shown the dynamic behavior similar in many aspects to that observed for the probes in our study.<sup>46</sup> The nitroxide labels attached at the beginning of the tail were more rigidly fixed than the labels located at the end of the tail. Moreover, our MD-simulated rotation times agree well with the effective correlation time of 1.5 ns for rotation of the Doxyl group of 14-Doxyl-PC in a DMPC bilayer measured using the time-resolved EPR technique.<sup>62</sup>

**Comparison with Experiments.** Several relative spectroscopic depth scales utilizing spin labels have been suggested for immersion depth measurements by using various spectroscopy techniques such as fluorescence,<sup>2,7</sup> EPR,<sup>9,11</sup> and NMR.<sup>13</sup> In fluorescence studies, quenching of a target fluorescence probe by a paramagnetic spin label depends on their relative positions within a membrane; therefore, penetration depth is commonly defined as the distance from a probe to the bilayer center.<sup>4,6</sup> In EPR methods, another paramagnetic agent such as Mn<sup>2+</sup> ion needs to be present to measure the distance between two spins so that the immersion depth is often considered as the distance from the bilayer surface to a spin-labeled site within a membrane.

The aim of the present study is to estimate the membrane depths of a series containing six spin labels (five *n*-Doxyls and Tempo) using MD simulations. A broad range of the spin labeling positions was considered, from the lipid headgroup up to the terminal carbons of the *sn*-2 lipid chain (Scheme 1). Table 1 compares the MD-estimated depths with the available experimental values. Figure 7 shows a comparison of the MD-estimated depths with those determined from the X-ray diffraction data of the unlabeled bilayer<sup>18</sup> and scaled according to the order parameter versus *sn*-2 carbon atom data derived from <sup>2</sup>H NMR<sup>19</sup> (Table 1). The depth of the spin labels attached to opposite ends of the lipid chain, at C-5 and C-14, agrees well with the depths of the corresponding unlabeled carbon atoms. However, some systematic upward deviations were observed for the spin labels attached to carbons C-7, C-10, and C-12. For 10-Doxyl, the deviation between the MD-estimated depth and the position of the unlabeled carbon atom C-10 is the largest and equals up to 4.2 Å. It is interesting that our MD-estimated membrane depths of 5- and 10-Doxyl labels correlate very well with the depths derived from the recent NMR experiments.<sup>13</sup> There is, however, some deviation between the depth of C-14 estimated by MD/X-ray and NMR techniques, Figure 7. We do not have firm evidence for

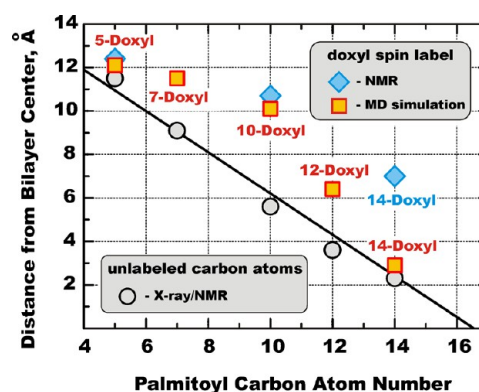


**Figure 7.** Comparison of experimental and MD-estimated depths. The MD-estimated depths of 5, 7, 10, 12, and 14-Doxyl labels (squares) are plotted versus the lipid chain carbon atom number. The MD-depths of 7, 10, and 12-Doxyls demonstrate systematic upward deviations from the calibration line derived from the carbon atom depths (circles) in the unlabeled *sn*-2 lipid chain based on the X-ray/NMR data.<sup>9,18,19</sup>

the origin of this deviation, but it could be related to the variations in lipid compositions used in different sets of experiments (DMPC and PSPC vesicles in the case of X-ray<sup>9,18</sup> and NMR,<sup>13</sup> respectively) and MD simulations (POPC bilayer).

The distance of the Tempo nitroxide group from the bilayer surface (approximated by the position of the cholines and assuming the positions of phosphorus = 0) derived by Pearson and Pascher<sup>18</sup> from X-ray diffraction data of DMPC crystals was found to be at 6–8 Å.<sup>9</sup> Assuming the thickness of the POPC leaflet to be 19.1 Å,<sup>21</sup> the depth of the Tempo label from the bilayer center is re-calculated at 11.1–13.1 Å. This value agrees with the major peak position of the Tempo group of 12.9 Å estimated in our MD simulations of the Tempo-PC/POPC system at the low spin probe concentration. Utilizing fluorescence quenching of a polar, lipid-attached NBD fluorophore by spin-labeled lipids, Abrams and London derived the depth of the Tempo nitroxide group to be 19.5 Å from the bilayer center.<sup>8</sup> This limiting depth value reported for the Tempo moiety, which places it almost near the membrane surface, can be explained by taking into account that such fluorescence quenching experiments typically utilize high concentrations of spin-labeled lipids in the membrane. Our MD simulations indicate that, indeed, the average depth of the Tempo group is shifted toward the membrane surface upon the increase of the concentration of Tempo-PC, reaching the value of 18.2 Å (Figure 5).

## SUMMARY AND PERSPECTIVE

In this Article, we have presented an MD study of a series of *n*-Doxyl-labeled lipids (Scheme 1) to investigate the structure, local mobility, and immersion depth distribution of the Doxyl spin moiety within a POPC bilayer. Our MD simulations demonstrate that the intrinsic thermal disorder of the bilayer (a broad range of lipid chain conformations) leads to the broad and heterogeneous distributions of the depths of the spin labels across the membrane normal (Figure 1). Nevertheless, the depth distributions of the Doxyl labels correlate well with the depths of the attachment carbon atoms in the unlabeled chain. We found that the immersion depth of the Doxyl labels attached at the C-5 and C-14 positions agrees very well with those of the corresponding unlabeled acyl chain carbon atoms



(Figure 3 and Table 1). When the Doxyl group was attached to the middle of the acyl chain (C-7, C-10, and C-12), some systematic upward deviations were observed, as can be seen in Figure 7. The largest difference of  $\sim 4$  Å between the immersion depth of the spin probe and the position of the unlabeled carbon atom was observed for the spin group of 10-Doxyl-PC.

Overall results of our MD study suggest that the distribution of the spin label within the model membrane is mainly dictated by the depth of the  $n$ -th chain carbon atom of the host phospholipid molecule. Because of its small size, the intrinsic properties of the Doxyl spin label, such as polarity and a hydrophobic/hydrophilic balance, play a minor role in favoring its membrane position. This behavior of the Doxyl probe, attached to POPC lipid molecules, differs from the membrane behavior of the spin labels, which were covalently attached to either alkylphospholipid analogues<sup>46</sup> or fatty acids.<sup>44,45</sup>

In contrast to  $n$ -Doxyl-PCs, the headgroup-labeled Tempo-PC lipids have shown a more complicated behavior in the model membrane. Our MD simulations revealed that, due to its hydrophobic nature, a Tempo group favors partitioning from the headgroup region deeper into the water-free region of the membrane. The average depth of the spin moiety also depends on the concentration of Tempo-PC lipids in the bilayer in the range of concentrations typical for fluorescence quenching experiments.<sup>8,12,13</sup> At low concentration of 11 mol % of bilayer labeling, the Tempo group favors residing at depths ranging from 12.9 Å (the major distribution peak position) to 14.4 Å (the center-of-weight of the distribution profile), as shown in Figure 5. In addition to the major population of the Tempo group partitioned deeply into the membrane, some minor subpopulation of the label is also observed at the outer bilayer interface (at  $\sim 26$ – $28$  Å from the center). The results of the MD simulations of the higher Tempo-PC concentration of 28 mol % suggest that the bulk character of the Tempo group results in significant broadening of its transverse membrane distribution so that the average label depth spans a range from 15.4 to 18.2 Å from the bilayer center. Thus, we argue that the average immersion depth of the Tempo quencher can be very sensitive to the concentration of Tempo-PCs in the membrane, which therefore becomes critical in the proper setup of depth-dependent fluorescence quenching experiments.

## ■ ASSOCIATED CONTENT

### ■ Supporting Information

Figures S1–S3 include the analyses from the MD simulations. Molecular dynamics topology of the spin-labeled lipids and coordinates of the equilibrated spin-labeled bilayer systems. This material is available free of charge via the Internet at <http://pubs.acs.org>.

## ■ AUTHOR INFORMATION

### Corresponding Author

\*E-mail: [a.v.kyrychenko@karazin.ua](mailto:a.v.kyrychenko@karazin.ua).

### Notes

The authors declare no competing financial interest.

## ■ ACKNOWLEDGMENTS

This work was performed using computational facilities of the joint computational cluster of SSI "Institute for Single Crystals" and Institute for Scintillation Materials of National Academy of Science of Ukraine incorporated into Ukrainian National Grid. The research was supported by National Institutes of Health

Grant GM-069783. A.K. also acknowledges support of Grant 0113U002426 of Ministry of Education and Science of Ukraine. We are grateful to Mr. M.A. Myers for his editorial assistance.

## ■ ABBREVIATIONS USED

POPC, 1-palmitoyl-2-oleoyl-*sn*-glycero-3-phosphocholine; PSPC, 1-palmitoyl-2-stearoyl-*sn*-glycero-3-phosphocholine; DMPC, 1,2-dimyristoyl-*sn*-glycero-3-phosphocholine; Tempo-PC, 1-palmitoyl-2-oleoyl-*sn*-glycero-3-phospho(TEMPO)-choline;  $n$ -Doxyl-PC, 1-palmitoyl-2-stearoyl-( $n$ -Doxyl)-*sn*-glycero-3-phosphocholine; MD simulation, molecular dynamics simulation; EPR, electron paramagnetic resonance; NMR, nuclear magnetic resonance; FRET, Förster resonance energy transfer; DA, distribution analysis; COM, center-of-mass

## ■ REFERENCES

- (1) Klug, C. S.; Feix, J. B. Methods and Applications of Site-Directed Spin Labeling EPR Spectroscopy. *Methods Cell Biol.* **2008**, *84*, 617–658.
- (2) Chattopadhyay, A.; London, E. Parallax Method for Direct Measurement of Membrane Penetration Depth Utilizing Fluorescence Quenching by Spin-Labeled Phospholipids. *Biochemistry* **1987**, *26* (1), 39–45.
- (3) Ladokhin, A. S. Distribution Analysis of Depth-Dependent Fluorescence Quenching in Membranes: A Practical Guide. In *Methods in Enzymology*; Ludwig Brand, M. L. J., Ed.; Academic Press: New York, 1997; Vol. 278, pp 462–473.
- (4) Ladokhin, A. S. Analysis of Protein and Peptide Penetration into Membranes by Depth-Dependent Fluorescence Quenching: Theoretical Considerations. *Biophys. J.* **1999**, *76*, 946–955.
- (5) Ladokhin, A. S. Evaluation of Lipid Exposure of Tryptophan Residues in Membrane Peptides and Proteins. *Anal. Biochem.* **1999**, *276* (2), 65–71.
- (6) London, E.; Ladokhin, A. S. Measuring the Depth of Amino Acid Residues in Membrane-Inserted Peptides by Fluorescence Quenching. *Curr. Top. Membr.* **2002**, *52*, 89–115.
- (7) Ladokhin, A. S.; Holloway, P. W.; Kostrzewska, E. G. Distribution Analysis of Membrane Penetration of Proteins by Depth-Dependent Fluorescence Quenching. *J. Fluoresc.* **1993**, *3* (3), 195–197.
- (8) Abrams, F. S.; London, E. Extension of the Parallax Analysis of Membrane Penetration Depth to the Polar Region of Model Membranes: Use of Fluorescence Quenching by a Spin-Label Attached to the Phospholipid Polar Headgroup. *Biochemistry* **1993**, *32* (40), 10826–10831.
- (9) Dalton, L. A.; McIntyre, J. O.; Fleischer, S. Distance Estimate of the Active Center of D- $\beta$ -Hydroxybutyrate Dehydrogenase from the Membrane Surface. *Biochemistry* **1987**, *26* (8), 2117–2130.
- (10) Ellena, J. F.; Archer, S. J.; Dominey, R. N.; Hill, B. D.; Cafiso, D. S. Localizing the Nitroxide Group of Fatty Acid and Voltage-Sensitive Spin-Labels in Phospholipid Bilayers. *Biochim. Biophys. Acta, Biomembr.* **1988**, *940* (1), 63–70.
- (11) Nielsen, R. D.; Che, K.; Gelb, M. H.; Robinson, B. H. A Ruler for Determining the Position of Proteins in Membranes. *J. Am. Chem. Soc.* **2005**, *127* (17), 6430–6442.
- (12) Al-Abdul-Wahid, M. S.; Neale, C.; Pomès, R. g.; Prosser, R. S. A Solution NMR Approach to the Measurement of Amphiphile Immersion Depth and Orientation in Membrane Model Systems. *J. Am. Chem. Soc.* **2009**, *131* (18), 6452–6459.
- (13) Chu, S.; Maltsev, S.; Emwas, A. H.; Lorigan, G. A. Solid-State NMR Paramagnetic Relaxation Enhancement Immersion Depth Studies in Phospholipid Bilayers. *J. Magn. Reson.* **2010**, *207* (1), 89–94.
- (14) Carmieli, R.; Papo, N.; Zimmermann, H.; Potapov, A.; Shai, Y.; Goldfarb, D. Utilizing ESEEM Spectroscopy to Locate the Position of Specific Regions of Membrane-Active Peptides within Model Membranes. *Biophys. J.* **2006**, *90* (2), 492–505.

- (15) Hubbell, W. L.; McConnell, H. M. Orientation and Motion of Amphiphilic Spin Labels in Membranes. *Proc. Natl. Acad. Sci. U.S.A.* **1969**, *64* (1), 20–27.
- (16) Godici, P. E.; Landsberger, F. R. Dynamic structure of lipid membranes. Carbon-13 nuclear magnetic resonance study using spin labels. *Biochemistry* **1974**, *13* (2), 362–368.
- (17) Fretten, P.; Morris, S. J.; Watts, A.; Marsh, D. Lipid-Lipid and Lipid-Protein Interactions in Chromaffin Granule Membranes: A Spin Label ESR Study. *Biochim. Biophys. Acta, Biomembr.* **1980**, *598* (2), 247–259.
- (18) Pearson, R. H.; Pascher, I. The Molecular Structure of Lecithin Dihydrate. *Nature* **1979**, *281*, 499–501.
- (19) Seelig, J.; Seelig, A. Lipid Conformation in Model Membranes and Biological Membranes. *Q. Rev. Biophys.* **1980**, *13* (1), 19–61.
- (20) Wiener, M. C.; White, S. H. Structure of a Fluid Dioleoylphosphatidylcholine Bilayer Determined by Joint Refinement of X-Ray and Neutron Diffraction Data. III. Complete Structure. *Biophys. J.* **1992**, *61* (2), 434–447.
- (21) Kučerka, N.; Tristram-Nagle, S.; Nagle, J. Structure of Fully Hydrated Fluid Phase Lipid Bilayers with Monounsaturated Chains. *J. Membr. Biol.* **2006**, *208* (3), 193–202.
- (22) Vogel, A.; Scheidt, H. A.; Huster, D. The Distribution of Lipid Attached Spin Probes in Bilayers: Application to Membrane Protein Topology. *Biophys. J.* **2003**, *85* (3), 1691–1701.
- (23) Mihailescu, M.; DVaswani, Rishi, G.; Jardón-Valadez, E.; Castro-Román, F.; Freitas, J. A.; Worcester, David, L.; Chamberlin, A. R.; Tobias, D. J.; White, S. H. Acyl-Chain Methyl Distributions of Liquid-Ordered and -Disordered Membranes. *Biophys. J.* **2011**, *100* (6), 1455–1462.
- (24) Braun, A. R.; Sachs, J. N. Extracting Experimental Measurables from Molecular Dynamics Simulations of Membranes. In *Annual Reports in Computational Chemistry*; Ralph, A. W., Ed.; Elsevier: New York, 2011; Vol. 7, pp 125–150.
- (25) Kučerka, N.; Holland, B. W.; Gray, C. G.; Tomberli, B.; Katsaras, J. Scattering Density Profile Model of POPG Bilayers As Determined by Molecular Dynamics Simulations and Small-Angle Neutron and X-ray Scattering Experiments. *J. Phys. Chem. B* **2011**, *116* (1), 232–239.
- (26) Heberle, F.; Pan, J.; Standaert, R.; Drazba, P.; Kučerka, N.; Katsaras, J. Model-Based Approaches for the Determination of Lipid Bilayer Structure from Small-Angle Neutron and X-ray Scattering Data. *Eur. Biophys. J.* **2012**, *41* (10), 875–890.
- (27) Kyrychenko, A.; Waluk, J. Distribution and Favorable Binding Sites of Pyrroloquinoline and Its Analogues in a Lipid Bilayer Studied by Molecular Dynamics Simulations. *Biophys. Chem.* **2008**, *136* (2–3), 128–135.
- (28) Jurkiewicz, P.; Cwiklik, L.; Jungwirth, P.; Hof, M. Lipid Hydration and Mobility: An Interplay between Fluorescence Solvent Relaxation Experiments and Molecular Dynamics Simulations. *Biochimie* **2012**, *94* (1), 26–32.
- (29) Garrido, L.; Pozuelo, J.; López-González, M.; Yan, G.; Fang, J.; Riande, E. Influence of the Water Content on the Diffusion Coefficients of Li<sup>+</sup> and Water Across Naphthalenic Based Copolyimide Cation-Exchange Membranes. *J. Phys. Chem. B* **2012**, *116* (38), 11754–11766.
- (30) Notman, R.; Anwar, J. Breaching the Skin Barrier—Insights from Molecular Simulation of Model Membranes. *Adv. Drug Delivery Rev.* **2013**, *65* (2), 237–250.
- (31) Kyrychenko, A.; Wu, F.; Thummel, R. P.; Waluk, J.; Ladokhin, A. S. Partitioning and Localization of Environment-Sensitive 2-(2'-Pyridyl)- and 2-(2'-Pyrimidyl)-indoles in Lipid Membranes: A Joint Refinement Using Fluorescence Measurements and Molecular Dynamics Simulations. *J. Phys. Chem. B* **2010**, *114* (42), 13574–13584.
- (32) Stepniewski, M.; Kepczynski, M.; Jamróz, D.; Nowakowska, M.; Rissanen, S.; Vattulainen, I.; Róg, T. Interaction of Hematoporphyrin with Lipid Membranes. *J. Phys. Chem. B* **2012**, *116* (16), 4889–4897.
- (33) Loura, L. M. S.; do Canto, A. M. T. M.; Martins, J. Sensing Hydration and Behavior of Pyrene in POPC and POPC/Cholesterol Bilayers: A Molecular Dynamics Study. *Biochim. Biophys. Acta, Biomembr.* **2013**, *1828* (3), 1094–1101.
- (34) Kyrychenko, A.; Tobias, D. J.; Ladokhin, A. S. Validation of Depth-Dependent Fluorescence Quenching in Membranes by Molecular Dynamics Simulation of Tryptophan Octyl Ester in POPC Bilayer. *J. Phys. Chem. B* **2013**, *117* (17), 4770–4778.
- (35) Kyrychenko, A.; Sevriukov, I. Y.; Syzova, Z. A.; Ladokhin, A. S.; Doroshenko, A. O. Partitioning of 2,6-Bis(1H-Benzimidazol-2-yl)-pyridine Fluorophore into a Phospholipid Bilayer: Complementary Use of Fluorescence Quenching Studies and Molecular Dynamics Simulations. *Biophys. Chem.* **2011**, *154* (1), 8–17.
- (36) Berger, O.; Edholm, O.; Jähnig, F. Molecular Dynamics Simulations of a Fluid Bilayer of Dipalmitoylphosphatidylcholine at Full Hydration, Constant Pressure, And Constant Temperature. *Biophys. J.* **1997**, *72* (5), 2002–2013.
- (37) Hermans, J.; Berendsen, H. J. C.; Van Gunsteren, W. F.; Postma, J. P. M. A Consistent Empirical Potential for Water-Protein Interactions. *Biopolymers* **1984**, *23* (8), 1513–1518.
- (38) Berendsen, H. J. C.; Postma, J. P. M.; van Gunsteren, W. F.; DiNola, A.; Haak, J. R. Molecular dynamics with coupling to an external bath. *J. Chem. Phys.* **1984**, *81* (8), 3684–3690.
- (39) Darden, T.; York, D.; Pedersen, L. Particle Mesh Ewald: An N × log(N) Method for Ewald Sums in Large Systems. *J. Chem. Phys.* **1993**, *98* (12), 10089–10092.
- (40) Hess, B.; Bekker, H.; Berendsen, H. J. C.; Fraaije, J. G. E. M. LINC: A Linear Constraint Solver for Molecular Simulations. *J. Comput. Chem.* **1997**, *18* (12), 1463–1472.
- (41) Van Der Spoel, D.; Lindahl, E.; Hess, B.; Groenhof, G.; Mark, A. E.; Berendsen, H. J. C. GROMACS: Fast, Flexible, and Free. *J. Comput. Chem.* **2005**, *26* (16), 1701–1718.
- (42) Humphrey, W.; Dalke, A.; Schulten, K. VMD: Visual Molecular Dynamics. *J. Mol. Graphics* **1996**, *14* (1), 33–38.
- (43) Bahlakeh, G.; Nikazar, M. Molecular Dynamics Simulation Analysis of Hydration Effects on Microstructure and Transport Dynamics in Sulfonated Poly(2,6-dimethyl-1,4-phenylene oxide) Fuel Cell Membranes. *Int. J. Hydrogen Energy* **2012**, *37* (17), 12714–12724.
- (44) Stimson, L.; Dong, L.; Karttunen, M.; Wisniewska, A.; Dutka, M.; Róg, T. Stearic Acid Spin Labels in Lipid Bilayers: Insight through Atomistic Simulations. *J. Phys. Chem. B* **2007**, *111* (43), 12447–12453.
- (45) Vartorelli, M. n. R.; Garay, A. S.; Rodrigues, D. E. Spin-Labeled Stearic Acid Behavior and Perturbations on the Structure of a Gel-Phase-Lipid Bilayer in Water: 5-, 12- and 16-SASL. *J. Phys. Chem. B* **2008**, *112* (51), 16830–16842.
- (46) Mravljak, J.; Konc, J.; Hodošček, M.; Šolmajer, T.; Pečar, S. Spin-Labeled Alkylphospholipids in a Dipalmitoylphosphatidylcholine Bilayer: Molecular Dynamics Simulations. *J. Phys. Chem. B* **2006**, *110* (51), 25559–25561.
- (47) Loura, L. M. S.; Prates Ramalho, J. P. Recent Developments in Molecular Dynamics Simulations of Fluorescent Membrane Probes. *Molecules* **2011**, *16*, 5437–5452.
- (48) Skaug, M. J.; Longo, M. L.; Faller, R. Computational Studies of Texas Red–1,2-Dihexadecanoyl-sn-glycero-3-phosphoethanolamine—Model Building and Applications. *J. Phys. Chem. B* **2009**, *113* (25), 8758–8766.
- (49) Skaug, M. J.; Longo, M. L.; Faller, R. The Impact of Texas Red on Lipid Bilayer Properties. *J. Phys. Chem. B* **2011**, *115* (26), 8500–8505.
- (50) Kyrychenko, A. A Molecular Dynamics Model of Rhodamine-Labeled Phospholipid Incorporated into a Lipid Bilayer. *Chem. Phys. Lett.* **2010**, *485* (1–3), 95–99.
- (51) Filipe, H. A. L.; Moreno, M. J.; Loura, L. M. S. Interaction of 7-Nitrobenz-2-oxa-1,3-diazol-4-yl-labeled Fatty Amines with 1-Palmitoyl, 2-Oleoyl-sn-glycero-3-phosphocholine Bilayers: A Molecular Dynamics Study. *J. Phys. Chem. B* **2011**, *115* (33), 10109–10119.
- (52) Loura, L. M. S.; Ramalho, J. P. P. Location and Dynamics of Acyl Chain NBD-Labeled Phosphatidylcholine (NBD-PC) in DPPC Bilayers. A Molecular Dynamics and Time-Resolved Fluorescence Anisotropy Study. *Biochim. Biophys. Acta, Biomembr.* **2007**, *1768* (3), 467–478.



- (53) Loura, L. M. S.; Fernandes, F.; Fernandes, A. C.; Ramalho, J. P. Effects of Fluorescent Probe NBD-PC on the Structure, Dynamics and Phase Transition of DPPC. A Molecular Dynamics and Differential Scanning Calorimetry Study. *Biochim. Biophys. Acta, Biomembr.* **2008**, *1778* (2), 491–501.
- (54) Orsi, M.; Sanderson, W. E.; Essex, J. W. Permeability of Small Molecules through a Lipid Bilayer: A Multiscale Simulation Study. *J. Phys. Chem. B* **2009**, *113* (35), 12019–12029.
- (55) Xiang, T. X. Translational Diffusion in Lipid Bilayers: Dynamic Free-Volume Theory and Molecular Dynamics Simulation. *J. Phys. Chem. B* **1998**, *103* (2), 385–394.
- (56) Vaz, W. L. C.; Clegg, R. M.; Hallmann, D. Translational Diffusion of Lipids in Liquid Crystalline Phase Phosphatidylcholine Multibilayers. A Comparison of Experiment with Theory. *Biochemistry* **1985**, *24* (3), 781–786.
- (57) Schwille, P.; Korch, J.; Webb, W. W. Fluorescence Correlation Spectroscopy with Single-Molecule Sensitivity on Cell and Model Membranes. *Cytometry* **1999**, *36* (3), 176–182.
- (58) Jóhárt, B.; Martinek, T. A. Performance of the General Amber Force Field in Modeling Aqueous POPC Membrane Bilayers. *J. Comput. Chem.* **2007**, *28* (12), 2051–2058.
- (59) Müller, T. J.; Müller-Plathe, F. Determining the Local Shear Viscosity of a Lipid Bilayer System by Reverse Non-Equilibrium Molecular Dynamics Simulations. *ChemPhysChem* **2009**, *10* (13), 2305–2315.
- (60) Håkansson, P.; Westlund, P. O.; Lindahl, E.; Edholm, O. A Direct Simulation of EPR Slow-Motion Spectra of Spin Labelled Phospholipids in Liquid Crystalline Bilayers Based on a Molecular Dynamics Simulation of the Lipid Dynamics. *Phys. Chem. Chem. Phys.* **2001**, *3* (23), 5311–5319.
- (61) Bemporad, D.; Luttmann, C.; Essex, J. W. Computer Simulation of Small Molecule Permeation Across a Lipid Bilayer: Dependence on Bilayer Properties and Solute Volume, Size, and Cross-Sectional Area. *Biophys. J.* **2004**, *87* (1), 1–13.
- (62) Gaffney, B. J.; Marsh, D. High-Frequency, Spin-Label EPR of Nonaxial Lipid Ordering and Motion in Cholesterol-Containing Membranes. *Proc. Natl. Acad. Sci. U.S.A.* **1998**, *95* (22), 12940–12943.